

SURFACE CLIMATE OF THE DARWIN-HATHERTON, TRANSANTARCTIC MOUNTAINS, WITH LINKS TO SYNOPTIC CIRCULATION.

Bob Noonan^{*1}, Peyman Zawar-Reza¹, Wendy Lawson²

¹Centre for Atmospheric Research, University of Canterbury, Christchurch, New Zealand

²Geography Department, University of Canterbury, Christchurch, New Zealand

[*bob.noonan@pg.canterbury.ac.nz](mailto:bob.noonan@pg.canterbury.ac.nz)

1. INTRODUCTION

Research concerning surface climate in the Transantarctic Mountains (TAM) has largely focused on the McMurdo Dry Valleys (MCM) region (Nylen et al., 2004; Speirs et al., 2012; Steinhoff et al., 2012). Mountains south of the MCM have largely been ignored due to logistics. Those studies that have concentrated on this southerly area have focused on the persistence and intensity of katabatic flow through TAM, the RIS airstream, and the connection with synoptic scale perturbations that circumnavigate the Ross Sea (Breckenridge et al., 1993; Bromwich et al., 1992; Bromwich, 1989; Parish and Bromwich, 1987; Seefeldt and Cassano, 2007; 2008; 2012; Steinhoff et al., 2009). While information about surface climate in the TAM can be gleaned from these studies, and from RIS based studies (Stearns et al., 1993; Reusch and Alley, 2004; Nigro et al., 2011), much remains unknown about variables such as air temperature, wind speed and relative humidity.

Zawar-Reza et al. (2010) provides the first non-MCM TAM study, focusing on the summertime valley boundary layer climate of the Darwin-Hatherton glacial system (DHGS) (Fig. 1). Their analysis reveals a diurnally oscillating wind regime in the DHGS, of downslope winds (akin to katabatic) starting in the late evening, switching to anabatic winds in the early afternoon.

The purpose of this research is to further progress knowledge of the annual surface climate in the section of the TAM, by distinguishing local climatic types, their frequency, and the synoptic pressure circulations under which they occur. We compare AWS data with a set of synoptic pressure states, formulated using simulated surface pressure (Polar Weather Research and Forecasting model (PWRF)), and the Self Organizing Maps Algorithm (SOM) which simplifies the array of simulated pressure states to a comprehensible number. PWRF and SOM are emergent tools for research in the RIS region (Nigro et al., 2011; Seefeldt and Cassano, 2007; 2008; 2012).

The DHGS is chosen to be the focus of this study also, as the climate record is comparatively extensive, with the Brown Hills AWS having been established since 2004.

This study is part of ongoing research into the surface mass balance (SMB) of the DHGS.

2. STUDY AREA AND DATA

Two main glaciers constitute the DHGS; the Darwin, which extends from the EAIS to the RIS, and the blue ice covered Hatherton which merges into it. These glaciers are members of a group of slow moving TAM glaciers.

The Brown Hills AWS is located in a small eastward sloping valley just to the north of the glacial system's outlet, but still encompassed within the DHGS (Fig. 1). The valley is ice free, with some isolated snow patches and frozen ponds; steep slopes are present to the north and south. Available glacier based AWS data (Lower Darwin, Marilyn, and Mulock AWS) are used to validate the use of Brown Hills data as proxy for glacial climate.

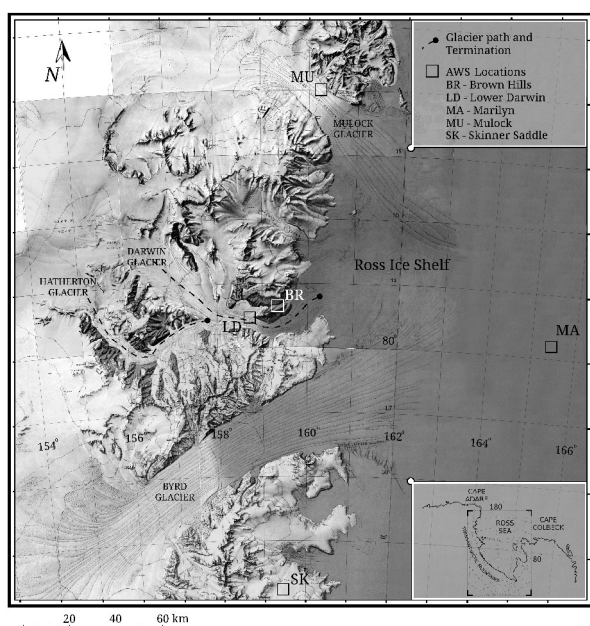


Fig. 1. Locations of the Darwin-Hatherton, Byrd, and Mulock glaciers, automatic weather stations (Brown Hills, Mulock, Lower Darwin, Marilyn, and Skinner Saddle, and lateral boundaries of PWRF simulations (insert, bottom left).

3. POLAR WRF

PWRF (v. 3.3.1) simulations are conducted for the period 2004 to 2011, with no data assimilation, using a simplified version of the Antarctic Mesoscale Prediction System's (AMPS) configuration

(<http://www.mmm.ucar.edu/rt/amps/information/configuration/configuration.html>). Boundary and initial conditions are supplied by National Center for Environmental Prediction/National Center for Atmospheric Research (NCEP/NCAR) re-analysis. Land use and topography information are taken from the default United States Geological Survey (USGS) dataset. Two grids (one-way nesting) cover the simulation area (Fig. 1, insert) (45km; 15 km resolution).

To ensure confidence in the simulated PWRF pressure data, validation is performed against measurements made by AWS located in the inner PWRF grid (<http://amrc.ssec.wisc.edu/aws/>).

The SOM algorithm is used to condense the simulated RIS SLP anomaly dataset, resulting in an output which reflects the continuum of SLP patterns in the region. By reducing the number of SLP patterns, it is anticipated that relationships which exist between the surface climate of the DHGS and synoptic circulation will become clearer. More information about SOM can be found in Sheridan and Lee (2011), and on the Helsinki University of Technology's Laboratory of Computer and Information Science website (<http://www.cis.hut.fi/research/som-research/nncr-programs.shtml>), from which the software (SOM_PAK) used in this study was sourced.

4. MEASURED SURFACE CLIMATE OF THE DHGS

4.1 ANNUAL

Downslope winds dominate the climate of the DHGS for the majority of the year; inferred from the clustering of measurements at $\sim 250^\circ$ (Fig. 2). Downslope winds are defined here as those winds that result from the combination of pressure gradient and katabatic forcing (Van den Broeke and Van Lipzig, 2003; Parish and Cassano, 2003). In mid November when the net radiation at the surface again becomes positive, downslope winds diminish in frequency, replaced by thermally driven upslope winds (Zawar-Reza et al., 2010). The intensity of these upslope winds is uniform, with wind speeds between 2 and 5 m s^{-1} . This uniformity contrasts to a background of rising wind speeds towards winter (defined here as May to

August, inclusive), in which average monthly speeds are maintained at $\sim 15 \text{ m s}^{-1}$, ranging from 0 to 35 m s^{-1} . Wind speeds in summer (December and January) do not exceed $\sim 25 \text{ m s}^{-1}$.

Temperature in the DHGS is kernlose (Fig. 2); summer temperatures range between -10°C to 5°C , cooling towards wintertime when mean monthly temperatures are relatively constant, lying near -25°C , but ranging from -5 to -40°C . The high variability observed of both the wind speed and air temperature in winter, reflects the fact that the system is tightly coupled to synoptic forcings (i.e. cold pool formations typically decouple some MCM regions from synoptic flow).

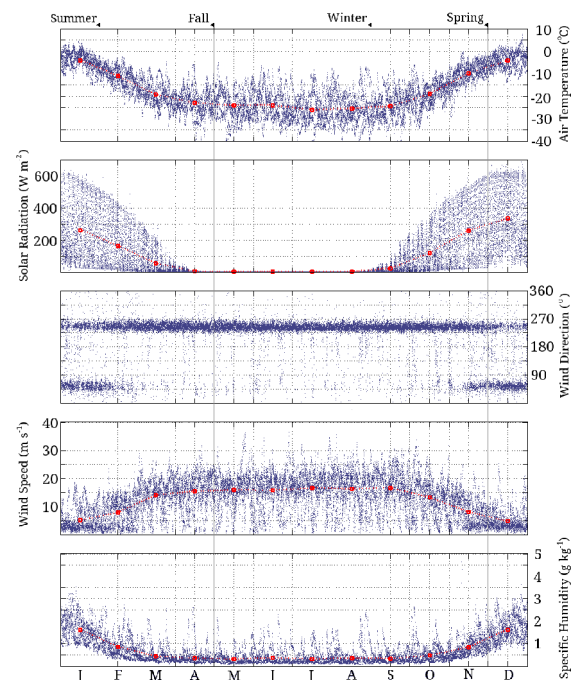


Fig. 2. Measured climate (air temperature, irradiance, wind direction, wind speed, specific humidity) for the Darwin-Hatherton glacial system, for the years 2005 to 2011 (ex. 2009). Displayed data are an amalgamation of all years, with x-axis markers indicating the mid month. Red dots are monthly averages. Data from the Brown Hills AWS.

Winter is a time of low humidity with a baseline level of $< 0.5 \text{ g kg}^{-1}$; very occasionally levels peak to 2.5 g kg^{-1} (Fig. 2). When mean air temperatures rise above -10°C in mid November, humidity levels become more uniformly spread between 1 to 3 g kg^{-1} .

Following this analysis, attention is solely given to the winter and summer climate, isolating the transitional climate associated with fall and spring, under the assumption that these intermediate seasons experience similar conditions to winter and summer, in addition to the transitional signal.

A high degree of correlation exists with the Lower Dawin AWS dataset for the summer of available data. Correlations with the datasets of the Mulock and Marilyn AWS indicate that surface climate at the location of the Brown Hills AWS would show increasing similarity to conditions on the DHGS as the year progresses from summer.

4.1 WINTER

Three other flow types can be discerned from the dataset in addition to the persistent downslope winds. 'Downslope' winds are clustered between 210 and 280° and 5 to 35 m s⁻¹ (<0.5 g kg⁻¹) (Fig. 3); no clear climate definition of downslope winds exist, but precedents have been established by other research (Nylen et al., 2004; Parish and Cassano, 2003). 'Local drainage' winds are separated from downslope winds using a 5 m s⁻¹ threshold following Nylen et al. (2004) and Seefeldt and Cassano (2007). Measurements from 'cold upslope' events lie between 0 and 90° and 0 to 5 m s⁻¹ (<0.5 g kg⁻¹), and 'warm' events between 90 and 270° and 0 to 10 m s⁻¹ (>0.5 g kg⁻¹).

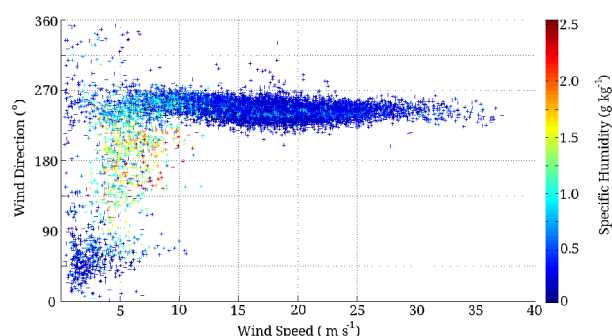


Fig. 3 Specific Humidity for the Darwin-Hatherton as a function of wind speed, direction for the winter (May to Aug). The magnitude of specific humidity is indicated by the color of the graph markers. Data from the Brown Hills AWS.

Downslope winds occur ~76 % of the time in winter, much higher than previous base line katabatic frequency estimates of 40-50% for the Byrd glacier (Breckenridge et al., 1993; Bromwich, 1989). For years with notable frequency anomalies (2008: 85%; 2011: 64%), differences are accounted for by fluctuations in warm events (average 14%). A tentative link exists between these warm events and positive snow surface height changes recorded at the location of the Skinner Saddle by Sinclair et al. (2010). Local drainage (1%) and cold upslope (2%) periods are minor influences; frequency variability is low.

4.1 SUMMER

Compared to the winter, summertime climate is more complex. Downslope winds (210 to 280°; 3 to 25 m s⁻¹) are still present (Fig. 4); however, as seen in Section 4.1.1, upslope winds (10 to 90°; 0 to 7 m s⁻¹) account for a substantial portion of the time. Now downslope winds occur sporadically between upslope flows, with durations ranging from the period of a morning to multiple days.

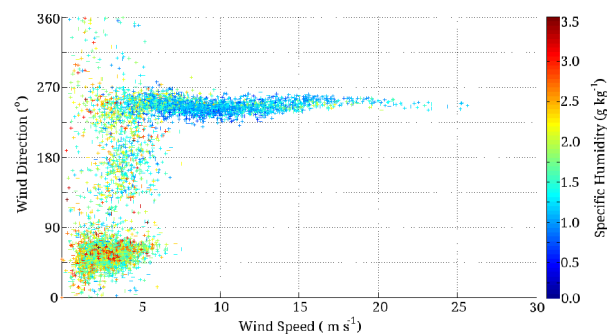


Fig. 4. As for Fig. 3, but using data from December to January.

Upslope flows appear to be a collection of several air flow sub-types, with near identical climatic conditions. While there are days characterised by morning downslope, and afternoon anabatic activity (Diurnal Anabatic) (Zawar-Reza et al., 2010), there are numerous periods where the duration of upslope winds is days to weeks (Persistent Anabatic). Some periods can be classed as precipitation events, following changes in wind direction, humidity, radiation and albedo.

A change from downslope winds results in a shift from dry, and gusty conditions to more humid, calmer conditions. The magnitude of temperature and humidity change are dependent on the upslope type.

Downslope winds account for ~33% of the time, persistent anabatic winds 35%, diurnal anabatic 16%, and precipitation 19%; frequency variability is high.

5. SYNOPTIC INFLUENCE ON SURFACE CLIMATE IN THE DHGS

5.1 SYNOPTIC CIRCULATION

The SLP anomaly SOM (Fig. 5) reflects common pressure states for the RIS region (Nigro et al., 2011). Frequencies derived for each node by season show a transition from weak synoptic circulations in summer (bottom left of SOM), to strong circulations in winter (top and right most of

SOM). Fall and spring have a more even distribution of pressure states; however, both distributions resemble more closely their preceding season. AWS measured surface pressure shows cohesion with the SOM, agreeing with Nigro et al. (2011) who found a strong correlation between synoptic circulation and pressure on the RIS.

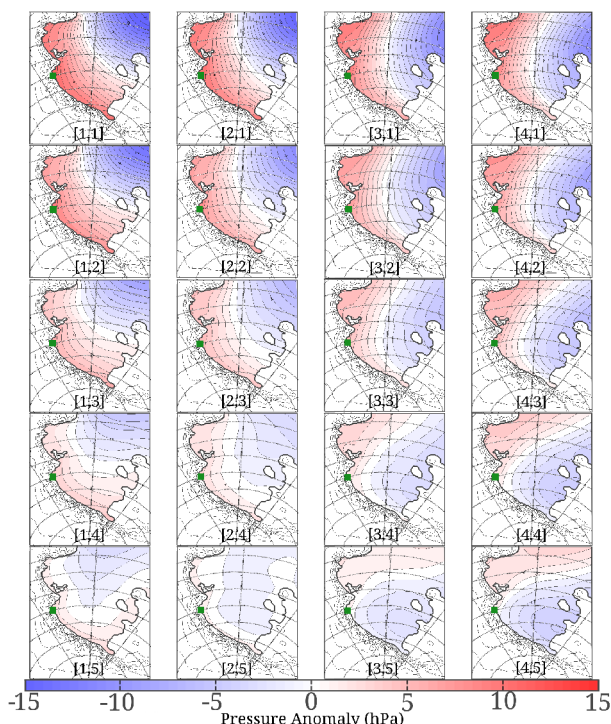


Fig. 5. SOM generated clusters of PWRP simulated surface level pressure anomaly (hPa) over the Ross Sea and Ice Shelf region, for the years 2004 to 2011. An approximate location of the DHGS is given by the green square.

Past research has found that the orientation and gradient of surface level pressure across the Ross Ice Shelf influences air flow in the region (Seefeldt et al., 2007; Breckenridge et al., 1993; Bromwich et al., 1992). Following Seefeldt et al. (2007), areas of the SOM map (Fig. 5) can be identified as being conducive to one of four RIS based wind systems. They define “Barrier winds” as those states which exhibit a pressure gradient on the RIS highest at the base of the TAM, extending out perpendicular to the range. This situation results from a low pressure system to the north of Cape Colbeck (Fig. 1), represented here by nodes in the top left corner of the SOM map. In this situation, stably stratified air builds up against the TAM leading to the development of a northward propagating geostrophic wind. Despite the pressure buildup at the base of the TAM, Seefeldt et al. (2007) found westerly winds were still evident at the location of Marilyn AWS,

indicating downslope drainage of Byrd Glacier. With eastward movement of the low nearer to Cape Colbeck (clockwise progression through the nodes of the SOM map), the orientation of the pressure gradient begins to enhance katabatic flow; “strong katabatic” flow occurs when the orientation of the gradient is parallel to the TAM, roughly the same as the glacial valleys (nodes [4,2] to [4,4]); “weaker katabatic” states (nodes [3,2] to [3,4]) are those with weaker gradients and less than parallel orientation. As the synoptic situation clears (movement of the low further east, reflected in a shift to the bottom left nodes) the synoptic assistance of katabatic flow lessens. A pressure gradient similarly orientated to the barrier situation, but weaker in gradient results in “light winds” for much of the RIS; Seefeldt et al. (2007) report light katabatic winds recorded at Marilyn AWS.

5.2 WINTER

In winter, downslope winds are present in all nodes, with high wind speeds for those measurements under “strong katabatic” circulation (max. 35 m s^{-1}), and lower speeds in “barrier” (max. 25 m s^{-1}) and “light wind” circulations (max. 30 m s^{-1}) (Fig. 6). Cold and warm events occur with greater frequency under “barrier” and “light wind” conditions. Calmer “local drainage” winds occur more in barrier situations.

The link between warm events and barrier situations, when air is being drawn from the ocean over West Antarctica rather than off the continent, is similar to the results of Sinclair et al. (2010) and also to Nicholas and Bromwich (2011) and Spinhirne et al. (2005), who both show an arc of cloud cover (effectively a perturbation to the radiation balance and source of precipitation), extending over the West Antarctic Ice Sheet towards the TAM.



Fig. 6. Frequency of each of the winter climate types identified in Section 4.1.2 as a function of SOM node.

5.3 SUMMER

The synoptic circulation in summer has a similar effect on downslope wind speeds as in winter, with wind strength increased under “strong katabatic” circulations, when compared to “barrier”. Maximum wind speeds are lower than winter due to surface heating and prevalence of lower intensity cyclones. Compared to the other types, downslope winds have greater presence in nodes representing higher intensity low centers (outer top and rightmost) (Fig. 7). Diurnally occurring anabatic winds are more frequent in nodes which support downslope flow (nodes [3,3] to [3,5] and [2,5]), while the persistent type has greater presence in nodes with weaker pressure gradients (nodes [2,4], [2,5] and [3,5]).

Downslope				Diurnal Anabatic			
3	1	3	1	0	2	5	0
5	3	4	2	1	3	4	1
7	6	7	2	4	8	10	3
4	8	8	6	3	7	12	5
4	7	14	5	2	11	12	6
Precipitation				Persistent Anabatic			
5	2	1	0	1	1	0	0
12	3	2	0	2	2	1	0
13	7	4	1	8	7	3	1
17	9	7	6	7	15	8	2
3	7	2	2	9	19	13	2

Fig. 7. Frequency of each of the summer climate types identified in Section 4.1.3 as a function of SOM node.

Precipitation events again occur under similar synoptic conditions to winter (nodes [1,2] to [1,4]), implying that synoptic conditions that produce precipitation remain similar year round.

The climate of the summertime downslope and anabatic flows contrasts starkly (downslope: gusty and dry, versus upslope: calm and humid). Given that the frequencies of these anabatic types are non trivial, understanding factors governing them should be an important part of climate and surface mass balance studies in this region.

6. ACKNOWLEDGEMENTS

The authors wish to thank Helicopters New Zealand, and the Christchurch City Council for funding this research, the Byrd Polar Institute and the Helsinki University of Technology's Laboratory of Computer and Information Science for the use of their software, and the University of Wisconsin, GNS, and NIWA for AWS data.

7. REFERENCES

Breckenridge, C. J., Radok, U., Stearns, C. R., and D. H. Bromwich, 1993: Katabatic winds along the Transantarctic Mountains. *Antarctic Meteorology and Climatology: Studies Based on Automatic Weather Stations*. Antarctic Research Series, Vol. 61. Bromwich D.H., and Stearns C.R., Eds. Amer. Geophys. Union: Washington, 69-92.

Bromwich, D. H. 1989: Satellite analyses of Antarctic katabatic wind behavior. *Bull. Amer. Meteor. Soc.*, **70**, 738-749.

Bromwich, D. H., Carrasco, J. F., and C. R. Stearns, 1992: Satellite observations of katabatic-wind propagation for great distances across the Ross Ice Shelf. *Mon. Wea. Rev.*, **120**, 1940-1949.

Nicolas, J. P., and D. H. Bromwich, 2011: Climate of West Antarctica and influence of marine air intrusions. *J. Climate*, **24**, 49-67.

Nigro, M. A., Cassano, J. J., and M. W. Seefeldt, 2011: A weather-pattern-based approach to evaluate the Antarctic Mesoscale Prediction System (AMPS) forecasts: Comparison to automatic weather station observations. *Wea. and Forecasting*, **26**, 184-198.

Nylen, T. H., Fountain, A. G., and P. T. Doran, 2004: Climatology of katabatic winds in the McMurdo Dry Valleys, Southern Victoria Land, Antarctica. *J. Geophys. Res.*, **109**, D03114, doi:10.1029/2003JD002927.

Parish, T. R., and D. H. Bromwich, 1987: The surface windfield over the Antarctic Ice Sheets. *Nature*, **328**, 51-54.

Parish, T. R., and J. J. Cassano, 2003: The role of katabatic winds on the Antarctic surface wind regime. *Mon. Wea. Rev.*, **131**, 317-333.

Reusch, D. B., and R. B. Alley, 2004: A 15-year West Antarctic climatology from six automatic weather station temperature and pressure records. *J. Geophys. Res.*, **109**, D04103, doi:10.1029/2003JD004178.

Seefeldt, M. W., Cassano, J. J., and T. R. Parish, 2007: Dominant regimes of the Ross Ice Shelf surface wind field during austral autumn 2005. *J. Appl. Meteor. Climatol.*, **46**, 1933-1955.

Seefeldt, M. W., and J. J. Cassano, 2008: An analysis of low-level jets in the greater Ross Ice Shelf

region based on numerical simulations. *Mon. Wea. Rev.*, **136**, 4188-4205.

Seefeldt, M. W., and J. J. Cassano, 2012: A description of the Ross Ice Shelf air stream (RAS) through the use of self-organizing maps (SOMs). *J. Geophys. Res.*, **117**, D09112, doi:10.1029/2011JD016857.

Sheridan, S. C., and C. C. Lee, 2011: The self-organizing map in synoptic climatological research. *Prog. Phys. Geogr.*, **35**, 109-119.

Sinclair, K. E., Bertler, N. A. N., and W. J. Trompeter, 2010: Synoptic controls on precipitation pathways and snow delivery to high-accumulation ice core sites in the Ross Sea region, Antarctica. *J. Geophys. Res.*, **115**, D22112, doi:10.1029/2010JD014383.

Speirs, J. C., McGowan, H. A., Steinhoff, D. F., and D. H. Bromwich, 2012: Regional climate variability driven by foehn winds in the McMurdo Dry Valleys, Antarctica. *Int. J. Climatol.* doi:10.1002/joc.3841.

Spinhirne, J. D., Palm, S. P., and W. D. Hart, 2005: Antarctica cloud cover for October 2003 from GLAS satellite lidar profiling. *Geophys. Res. Lett.*, **32**, L22S05, doi:10.1029/2005GL023782.

Stearns, C. R., Keller, L. M., Weidner, G. A., and M. Sievers, 1993: Monthly mean climatic data for Antarctic automatic weather stations. *Antarctic Meteorology and Climatology: Studies Based on Automatic Weather Stations*. Antarctic Research Series, Vol. 61. Bromwich D.H., and Stearns C.R., Eds. Amer. Geophys. Union: Washington, 1-21.

Steinhoff, D. F., Bromwich, D. H., and A. Monaghan, 2012: Dynamics of the foehn mechanism in the McMurdo Dry Valleys of Antarctica from Polar WRF. *Q. J. R. Meteor. Soc.* doi:10.1002/qj.2038.

Van den Broeke, M. R., and N. P. M. Van Lipzig, 2003: Factors Controlling the Near-Surface Wind Field in Antarctica. *Mon. Wea. Rev.*, **131**, 733-743.

Zawar-Reza, P., George, S., Storey, B., and W. Lawson, 2010: Summertime boundary layer winds over the Darwin–Hatherton glacial system, Antarctica: observed features and numerical analysis. *Antarct. Sci.*, **22**, 619-632.